

Multi-phase Vectorial Control of Synchronous Motors with Currents and Voltages Saturations

Marco Fei and Roberto Zanasi

Abstract—This paper deals with the torque control of m_s -phase synchronous machines where the first odd harmonics below m_s are injected. A new vectorial approach to describe the voltage and current limits is proposed. Starting from the transformed dynamic equations and using the voltage and current constraints, the optimal current references is obtained. It holds for an arbitrary number of star connected phases and an arbitrary shape of the rotor flux. Some simulation results for a 7-phase motor validate the proposed control law.

I. INTRODUCTION

Multi-phase machines offer some advantages and greater number of degrees of freedom compared to three-phase machines, see [2] and [3]. One of these advantages is the higher torque-to-volume ratio due to the injection of higher order current harmonics for the machines with concentrated winding and nearly rectangular back-emf, see [1], [4], [5]. In [6] and [7] the effects of the voltage and current limits on the third harmonic injection are considered. Almost all the abovementioned papers consider specific motors with 5 or 7 phases where only the first and the third current harmonics are injected. Moreover although the amplitude of the injected harmonics is tied to the harmonic spectrum of the back-emf, it is not clear how the current references are obtained.

This paper, which is an extension of [8], uses a new vectorial approach to obtain the optimal current references considering the voltage and current limits. The approach is as general as possible and it is suitable for machines with an arbitrary odd number of star-connected phases and an arbitrary shape of the rotor flux.

The paper is organized as follows. Sec. II shows the details of the dynamic model of the multi-phase synchronous motors. In Sec. III the current and voltage constraints are presented and their effects onto the torque producing capability are shown in Sec. IV and Sec. V. The proposed torque control is given in Sec. VI. Some simulation results are presented in Sec. VII and conclusions are given in Sec. VIII.

A. Notations

The full and diagonal matrices will be denoted as follows:

$$\begin{bmatrix} R_{11} & R_{12} & \dots & R_{1m} \\ R_{21} & R_{22} & \dots & R_{2m} \\ \vdots & \vdots & \ddots & \vdots \\ R_{n1} & R_{n2} & \dots & R_{nm} \end{bmatrix}, \quad \begin{bmatrix} R_1 & & \\ & R_2 & \\ & & \ddots \\ & & & R_n \end{bmatrix}$$

The symbols $\begin{bmatrix} R_i \\ \vdots \\ R_n \end{bmatrix}$ and $\begin{bmatrix} R_i & & \\ & R_i & \\ & & \ddots \\ & & & R_n \end{bmatrix}$ will denote the column and row matrices. The symbol $\sum_{n=a:d}^b c_n = c_a + c_{a+d} + c_{a+2d} + \dots$ will be

M. Fei and R. Zanasi are with the DII, University of Modena and Reggio Emilia, Via Vignolesse 905, 41100 Modena, Italy, e-mail: {marco.fei, roberto.zanasi}@unimore.it.

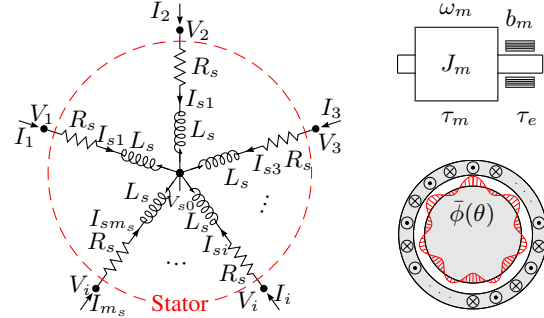


Fig. 1. Basic structure of a star-connected multi-phase synchronous motor.

used to represent the sum of a succession of numbers c_n where the index n ranges from a to b with increment d .

II. ELECTRICAL MOTORS MODELING

The basic structure of a permanent magnet synchronous motor with an *odd* number m_s of concentrated winding in star connection is shown in Fig. 1 and its parameters are shown in Fig. 2. A complex and reduced model in the rotating frame $\bar{\Sigma}_\omega$ can be obtained using the following reduced and complex transformation matrix ${}^t\bar{\mathbf{T}}_{\omega N} \in \mathbb{C}^{m_s \times \frac{m_s-1}{2}}$:

$${}^t\bar{\mathbf{T}}_{\omega N} = \sqrt{\frac{2}{m_s}} \begin{bmatrix} e^{jk(\theta - h\gamma_s)} \\ \vdots \\ e^{jk(\theta - h\gamma_s)} \end{bmatrix}_{0:m_s-1}^k \quad \begin{bmatrix} 1 \\ \vdots \\ 1 \end{bmatrix}_{1:2:m_s-2} \quad (1)$$

Using this transformation, and the POG modeling technique, see [9] and [10] one obtains the dynamic model reported in Fig. 3. The transformed system $\bar{\mathcal{S}}_\omega$ expressed in the complex reduced rotating frame $\bar{\Sigma}_\omega$ has the following form:

$$\begin{bmatrix} \omega \bar{\mathbf{L}}_s & \mathbf{0} \\ \mathbf{0} & J_m \end{bmatrix} \begin{bmatrix} \omega \dot{\bar{\mathbf{I}}}_s \\ \dot{\bar{\omega}}_m \end{bmatrix} = - \begin{bmatrix} \omega \bar{\mathbf{Z}}_s & \omega \bar{\mathbf{K}}_{\tau N} \\ -\omega \bar{\mathbf{K}}_{\tau N}^* & b_m \end{bmatrix} \begin{bmatrix} \omega \bar{\mathbf{I}}_s \\ \bar{\omega}_m \end{bmatrix} + \begin{bmatrix} \omega \bar{\mathbf{V}}_s \\ -\tau_e \end{bmatrix}. \quad (2)$$

The original m_s -dimension model is transformed and reduced to a $(m_s-1)/2$ -dimension complex model $\bar{\mathcal{S}}_\omega$ in the rotating frame $\bar{\Sigma}_\omega$. In this frame the m_s -phase motor can be seen as a set of $(m_s-1)/2$ independent electrical machines, rotating at different velocity $k\omega_m$, each one working within a complex subspace $\bar{\Sigma}_{\omega k}$ with $k \in \{1 : 2 : m_s - 2\}$. The complex matrix $\omega \bar{\mathbf{Z}}_s = \omega \bar{\mathbf{R}}_s + \omega \bar{\mathbf{L}}_s \omega \bar{\mathbf{J}}_s$ in (2) is defined as:

$$\omega \bar{\mathbf{Z}}_s = \begin{bmatrix} \omega \bar{\mathbf{Z}}_{sk} \\ \vdots \\ \omega \bar{\mathbf{Z}}_{sk} \end{bmatrix}_{1:2:m_s-2}^k = \begin{bmatrix} R_s + jp k \omega_m L_{sk} \\ \vdots \\ R_s + jp k \omega_m L_{sk} \end{bmatrix}_{1:2:m_s-2} \quad (3)$$

where $L_{sk} = L_s + M_{s0} \left(\frac{m_s}{2} a_{Mk} - 1 \right)$. Note that, according to [4], in (3) the first $m_s - 2$ odd components $a_{Mk} M_{s0}$ of the mutual inductance (see Fig. 2) are considered. The

m_s	number of motor phases
p	number of polar expansions
θ, θ_m	electric and rotor angular positions: $\theta = p\theta_m$
ω, ω_m	electric and rotor angular velocities: $\omega = p\omega_m$
R_s	i -th stator phase resistance
L_s	i -th stator phase self induction coefficient
M_{s0}	maximum value of the stator mutual inductance
M_{hi}	mutual induction coefficient between the phases h and i $M_{hi} = M_{s0} \sum_{n=1:2}^{m_s-2} a_{Mn} \cos(n(h-i)\gamma_s)$
J_m	rotor moment of inertia
b_m	rotor linear friction coefficient
τ_m	electromotive torque acting on the rotor
τ_e	external load torque acting on the rotor
γ_s	basic angular displacement ($\gamma_s = 2\pi/m_s$)
$\phi_c(\theta)$	total rotor flux chained with stator phase 1
φ_c	maximum value of function $\phi_c(\theta)$
$\bar{\phi}(\theta)$	normalized total rotor flux: $\bar{\phi}(\theta) = \frac{\phi_c(\theta)}{\varphi_c} = \sum_{n=1:2}^{\infty} a_i \cos(n\theta)$

Fig. 2. Variables and parameters of the multi-phase synchronous motor.

transformed torque vector $\omega \mathbf{K}_{\tau N}$ is function of the electric angle θ and the coefficients a_n of the flux Fourier series shown in Fig. 2. It can be shown, see [11], that when the normalized rotor flux is characterized by the first odd $m_s - 2$ harmonics the transformed torque vector $\omega \mathbf{K}_{\tau}$ is constant:

$$\omega \bar{\mathbf{K}}_{\tau N} = \left[\left[\bar{K}_{\tau k} \right] \right]_{1:2:m_s-2}^k = \left[\left[K_{dk} + jK_{qk} \right] \right]_{1:2:m_s-2}^k = jp\varphi_c \sqrt{\frac{m_s}{2}} \left[\left[ka_k \right] \right]_{1:2:m_s-2}^k \quad (4)$$

and each component $\bar{K}_{\tau k}$ is defined by the coefficient a_n of the same order k . According to the magnetic co-energy method, the motor torque τ_m and the back-electromotive force $\omega \bar{\mathbf{E}}$ are:

$$\tau_m = \Re \left(\omega \bar{\mathbf{K}}_{\tau N}^* \omega \bar{\mathbf{I}}_s \right), \quad \omega \bar{\mathbf{E}} = \omega \bar{\mathbf{K}}_{\tau N} \omega_m. \quad (5)$$

In [1] and [4] it is shown that it is possible to increase the motor torque of a multi phase motor by injecting odd harmonics with order below m_s . Let us now consider the case of balanced voltage and current stator vectors ${}^t \mathbf{V}_s$ and ${}^t \mathbf{I}_s$ composed by the first $(m_s - 1)/2$ harmonics:

$${}^t \mathbf{V}_s = \left[\left[V_{sh} \right] \right]_{1:m_s}^h = \sum_{k=1:2}^{m_s-2} \left[\left[V_{mk} \cos(k\theta - k(\theta_{vk} - (h-1)\gamma_s)) \right] \right]_{1:m_s}^h \quad (6)$$

$${}^t \mathbf{I}_s = \left[\left[I_{sh} \right] \right]_{1:m_s}^h = \sum_{k=1:2}^{m_s-2} \left[\left[I_{mk} \cos(k\theta - k(\theta_{ik} - (h-1)\gamma_s)) \right] \right]_{1:m_s}^h, \quad (7)$$

where V_{mk} and I_{mk} are the amplitude of the balanced harmonics components of order k and θ_{vk}, θ_{ik} are proper initial phase shifts. The transformed current and voltage vectors $\omega \bar{\mathbf{I}}_s = {}^t \bar{\mathbf{T}}_{\omega N}^* {}^t \mathbf{I}_s$ and $\omega \bar{\mathbf{V}}_s = {}^t \bar{\mathbf{T}}_{\omega N}^* {}^t \mathbf{V}_s$ are:

$$\omega \bar{\mathbf{V}}_s = \left[\left[\bar{V}_{sk} \right] \right]_{1:2:m_s-2}^k = \left[\left[V_{dk} + jV_{qk} \right] \right]_{1:2:m_s-2}^k = \sqrt{\frac{m_s}{2}} \left[\left[V_{mk} e^{jk\theta_{vk}} \right] \right]_{1:2:m_s-2}^k \quad (8)$$

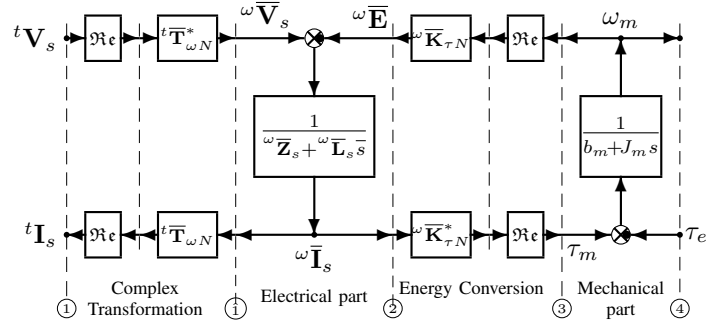


Fig. 3. POG scheme of a multi-phase electrical motor in the reduced complex rotating frame $\bar{\Sigma}_\omega$.

$$\omega \bar{\mathbf{I}}_s = \left[\left[\bar{I}_{sk} \right] \right]_{1:2:m_s-2}^k = \left[\left[I_{dk} + jI_{qk} \right] \right]_{1:2:m_s-2}^k = \sqrt{\frac{m_s}{2}} \left[\left[I_{mk} e^{jk\theta_{ik}} \right] \right]_{1:2:m_s-2}^k \quad (9)$$

where I_{dk}, I_{qk}, V_{dk} and V_{qk} are, respectively, the *direct* and *quadrature* components of the current and voltage vectors \bar{I}_{sk} and \bar{V}_{sk} . Expressions (8) and (9) show that the harmonics of order k and amplitude V_{mk} and I_{mk} in (6) and (7) are transformed into vectors \bar{V}_{sk} and \bar{I}_{sk} with modulus $V_{Mk} = \sqrt{\frac{m_s}{2}} V_{mk}$ and $I_{Mk} = \sqrt{\frac{m_s}{2}} I_{mk}$ which move in the complex subspace $\bar{\Sigma}_{\omega k}$. In other words each harmonic of order k is related to the fictitious electrical machine rotating at the same frequency $k\omega_m$ and characterized by the k -th coefficient of the rotor flux. Substituting (4) and (9) in (5) the motor torque can be rewritten as:

$$\tau_m = p\varphi_c \sqrt{\frac{m_s}{2}} \sum_{k=1:2}^{m_s-2} ka_k I_{qk}. \quad (10)$$

This equation shows the dependence of torque τ_m on the quadrature components I_{qk} of the current vectors \bar{I}_{sk} . From (10) it is clear that the torque production capability of the machine increases injecting the odd harmonics with order below to m_s . Moreover the amplitude of the injected harmonics is tied to the harmonic spectrum of the rotor flux (it is usefull to apply high I_{qk} in subspaces with high components ka_k).

III. MULTI HARMONICS CONSTRAINTS

The amplitudes of components V_{sh} and I_{sh} of the voltage and current vectors ${}^t \mathbf{V}_s$ and ${}^t \mathbf{I}_s$ in (6) and (7) are bounded, respectively, by the maximum voltage V_{max} of the inverter DC link and the maximum rated current I_{max} , therefore the following constraints hold:

$$\sum_{k=1:2}^{m_s-2} V_{mk} \leq V_{max}, \quad \sum_{k=1:2}^{m_s-2} I_{mk} \leq I_{max}. \quad (11)$$

Defining the vectors $\mathbf{V}_M, \mathbf{I}_M$ and $\mathbf{K}_\tau \in \mathbb{R}^{\frac{m_s-1}{2}}$ as:

$$\mathbf{V}_M = \left[\left[|\bar{V}_{sk}| \right] \right]_{1:2:m_s-2}^k, \quad \mathbf{I}_M = \left[\left[|\bar{I}_{sk}| \right] \right]_{1:2:m_s-2}^k, \quad \mathbf{K}_\tau = \left[\left[|\bar{K}_{\tau k}| \right] \right]_{1:2:m_s-2}^k$$

the voltage and current constraints (11), multiplied by constant $\sqrt{\frac{m_s}{2}}$, can be rewritten as a 1-norm constraint on

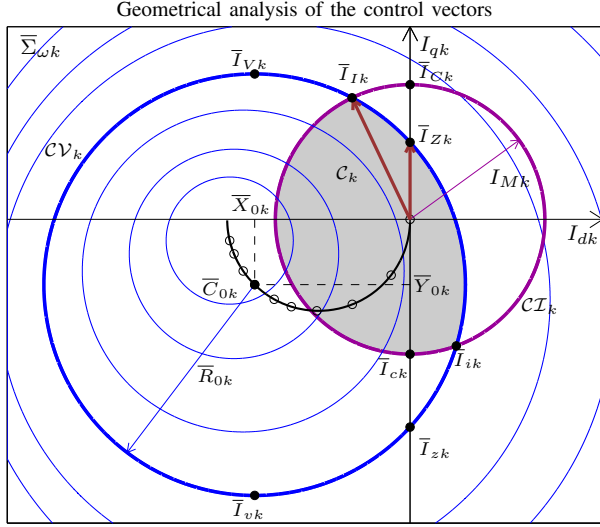


Fig. 4. Maximum current circles \mathcal{CV}_k and \mathcal{CT}_k in complex subspace Σ_{ω_k} .

vectors \mathbf{V}_M and \mathbf{I}_M :

$$\|\mathbf{V}_M\|_1 = \sum_{k=1:2}^{m_s-2} V_{Mk} \leq \sqrt{\frac{m_s}{2}} V_{max} = V_{\bar{M}}, \quad (12)$$

$$\|\mathbf{I}_M\|_1 = \sum_{k=1:2}^{m_s-2} I_{Mk} \leq \sqrt{\frac{m_s}{2}} I_{max} = I_{\bar{M}}, \quad (13)$$

where $V_{Mk} = \sqrt{\frac{m_s}{2}} V_{mk}$ and $I_{Mk} = \sqrt{\frac{m_s}{2}} I_{mk}$ are the moduli of vectors \bar{V}_{sk} and \bar{I}_{sk} , respectively.

In the design of the control law there are some degrees of freedom that will be used to decide how to distribute the maximum voltage $V_{\bar{M}}$ and current $I_{\bar{M}}$ into the components V_{Mk} and I_{Mk} to satisfy the constraints (12) and (13). In the next sections it will be shown how this defines in each subspace Σ_{ω_k} a specific operative zone that modifies the torque producing capability of the subspace.

IV. VECTORIAL CONTROL

In steady-state condition, the dynamic equation of the electrical part is $\omega \bar{\mathbf{V}}_s = -\omega \bar{\mathbf{Z}}_s \omega \bar{\mathbf{I}}_s - \omega \bar{\mathbf{K}}_\tau \omega_m$ which is equivalent to the following $(m_s - 1)/2$ equations of the complex subspaces Σ_{ω_k} :

$$\bar{V}_{sk} = -\bar{Z}_{sk} \bar{I}_{sk} - j K_{qk} \omega_m, \quad \bar{Z}_{sk} = R_s + j k p \omega_m L_{sk}. \quad (14)$$

The voltage constraint $\sqrt{V_{dk}^2 + V_{qk}^2} \leq V_{Mk}$ in the subspace Σ_{ω_k} can be rewritten as follows:

$$(I_{dk} - X_{0k})^2 + (I_{qk} - Y_{0k})^2 \leq R_{0k}^2 \quad (15)$$

$$\text{where } R_{0k}(\omega_m) = |\bar{R}_{0k}|_{|\bar{V}_{sk}|=V_{Mk}} = \frac{V_{Mk}}{|\bar{Z}_{sk}|} \quad (16)$$

$$X_{0k}(\omega_m) = \text{Re}(\bar{C}_{0k}) = \frac{-K_{qk} k p \omega_m^2 L_{sk}}{|\bar{Z}_{sk}|^2} \quad (17)$$

$$Y_{0k}(\omega_m) = \text{Im}(\bar{C}_{0k}) = \frac{-K_{qk} \omega_m R_s}{|\bar{Z}_{sk}|^2}. \quad (18)$$

Relation (15) is the mathematical expression of the maximum voltage circle \mathcal{CV}_k corresponding to the value V_{Mk} that

satisfies the voltage constraint (12). The terms $\bar{C}_{0k}(\omega_m) = X_{0k} + j Y_{0k}$ and $R_{0k}(\omega_m)$ represent the center and the radius of the maximum voltage circle \mathcal{CV}_k . These terms are function of the parameter ω_m . When velocity ω_m increases the radius R_{0k} of circle \mathcal{CV}_k decreases and its center \bar{C}_{0k} moves in the complex plane Σ_{ω_k} on a circle with center in $(\frac{-K_{qk}}{2 k p L_{sk}}, 0)$ and radius $\frac{K_{qk}}{2 k p L_{sk}}$. The current vector \bar{I}_{sk} satisfies the voltage constraint only if its modulus is inside the maximum voltage circle \mathcal{CV}_k . The current vector \bar{I}_{sk} must stay inside the maximum circle \mathcal{CT}_k having center in the origin and radius I_{Mk} and satisfying the current constraint (13):

$$I_{dk}^2 + I_{qk}^2 \leq I_{Mk}^2. \quad (19)$$

A graphical representation of the voltage and current circles \mathcal{CV}_k and \mathcal{CT}_k in the complex plane Σ_{ω_k} for a particular value of ω_m is shown in blue and violet in Fig. 4. The intersection zone \mathcal{C}_k between the two circles, shown in grey in Fig. 4, represents the area in which both the voltage and current constraints are satisfied. Subtracting equation (19) from equation (15) one obtains the following relation:

$$-2X_{0k}I_{dk} - 2Y_{0k}I_{qk} + X_{0k}^2 + Y_{0k}^2 - R_{0k}^2 + I_{Mk}^2 = 0.$$

Using this relation together with (19), one obtains the intersection points \bar{I}_{Ik} and \bar{I}_{ik} of circle \mathcal{CV}_k with circle \mathcal{CT}_k :

$$\bar{I}_{I,ik} = \frac{Y_{0k}}{|\bar{C}_{0k}|} \left[\frac{X_{0k} P_k}{|\bar{C}_{0k}|} \pm \sqrt{I_{Mk}^2 - \frac{Y_{0k}^2 P_k^2}{|\bar{C}_{0k}|^2}} \right] \left(1 - j \frac{X_{0k}}{Y_{0k}} \right) + j P_k \quad (20)$$

where $P_k = \frac{|\bar{C}_{0k}|^2 - R_{0k}^2 + I_{Mk}^2}{2Y_{0k}}$. The coordinates of the other points shown in Fig. 4 are:

$$\bar{I}_{V_k}(\omega_m) = X_{0k}(\omega_m) + j Y_{0k}(\omega_m) + j R_{0k}(\omega_m) \quad (21)$$

$$\bar{I}_{Z_k}(\omega_m) = j Y_{0k}(\omega_m) + j \sqrt{R_{0k}^2(\omega_m) - X_{0k}^2(\omega_m)} \quad (22)$$

$$\bar{I}_{Ck} = j I_{Mk} \quad (23)$$

$$\bar{I}_{ck} = -j I_{Mk} \quad (24)$$

$$\bar{I}_{z_k}(\omega_m) = j Y_{0k}(\omega_m) - j \sqrt{R_{0k}^2(\omega_m) - X_{0k}^2(\omega_m)} \quad (25)$$

$$\bar{I}_{v_k}(\omega_m) = j Y_{0k}(\omega_m) - j R_{0k}(\omega_m) \quad (26)$$

Note that the coordinates of all points shown in Fig. 4 are function of the components V_{Mk} and I_{Mk} . The torque τ_{mk} generated in the subspace Σ_{ω_k} can be provided using only the current $\bar{I}_{sk} \in \mathcal{C}_k$. Two main control laws can be used:

- 1) *field oriented control* where the direct component of the current vector is zero $\bar{I}_{sk} = \max \{ \bar{I}_{Ck}, \bar{I}_{Zk} \} \in \mathcal{C}_k$;
- 2) *flux weakening control* where also the direct component I_{dk} is used: $\bar{I}_{sk} = \max \{ \bar{I}_{v_k}, \bar{I}_{Ik} \} \in \mathcal{C}_k$.

In Fig. 4 the points \bar{I}_{Ck} and \bar{I}_{z_k} cannot be used in the control because they do not satisfy the constraints (\bar{I}_{Ck} and $\bar{I}_{z_k} \notin \mathcal{C}_k$). Using the field oriented control the operation point is $\bar{I}_{sk} = \bar{I}_{Zk}$, while using the flux weakening control the operation point is $\bar{I}_{sk} = \bar{I}_{Ik}$.

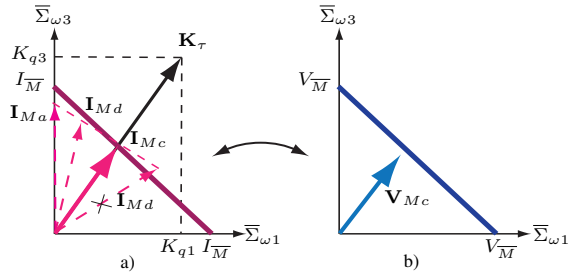


Fig. 5. Minimum dissipation constraints, $m_s = 5$: a) current, b) voltage.

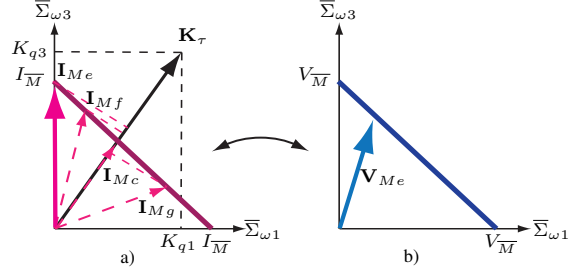


Fig. 6. Maximum torque constraints, $m_s = 5$: a) current, b) voltage.

V. CONSTRAINTS DISTRIBUTION

The torque can be provided using only the current vectors \bar{I}_{sk} inside the intersection zone \mathcal{C}_k of the maximum voltage and current limits, therefore the voltage and current limits determine the torque producing capability of the subspace $\bar{\Sigma}_{\omega_k}$. For a given ω_m , it is possible to modulate the components V_{Mk} and I_{Mk} in each subspace $\bar{\Sigma}_{\omega_k}$ in order to increase or decrease the maximum voltage and current circles \mathcal{CV}_k and \mathcal{CI}_k satisfying the constraints (12) and (13). For a 5-phase motor, the current and voltage 1-norm constraints can be represented as planes in \mathbb{R}^2 as shown in Fig. 5 and Fig. 6. From (5) it is clear that the torque τ_m is tied to the scalar product of \mathbf{K}_τ and \mathbf{I}_M and for this reason the vector \mathbf{K}_τ has been reported in the current 1-norm constraint of Fig. 5.a and Fig. 6.a. The torque control law described in the next section is a generalization, for a m_s -phase machine, of the following two cases of constraints distribution for a 5-phase machine:

Case 1) The optimal distribution of the current constraint minimizing the power dissipation is reported in Fig. 5.a. The vector \mathbf{I}_{Md} does not satisfy the current constraint, therefore this distribution cannot be used. The scalar product of the three vectors \mathbf{I}_{Ma} , \mathbf{I}_{Mb} and \mathbf{I}_{Mc} with the vector \mathbf{K}_τ is the same but the vectors \mathbf{I}_{Ma} and \mathbf{I}_{Mb} do not minimize the power dissipation because their moduli are greater than the modulus of \mathbf{I}_{Mc} . Therefore the current constraint vector which minimizes the power dissipation is the vector \mathbf{I}_{Mc} with the minimum modulus parallel to \mathbf{K}_τ . The voltage vector \mathbf{V}_{Mc} related to the current vector \mathbf{I}_{Mc} is reported in Fig. 5.b.

Case 2) The optimal distribution of the current constraint maximizing the torque τ_m is reported in Fig. 6.a. The vectors \mathbf{I}_{Mc} , \mathbf{I}_{Mf} and \mathbf{I}_{Mg} do not maximize the torque because their projections onto \mathbf{K}_τ are smaller than the projection of vector \mathbf{I}_{Me} . The vector $\mathbf{I}_M = \mathbf{I}_{Me}$ that

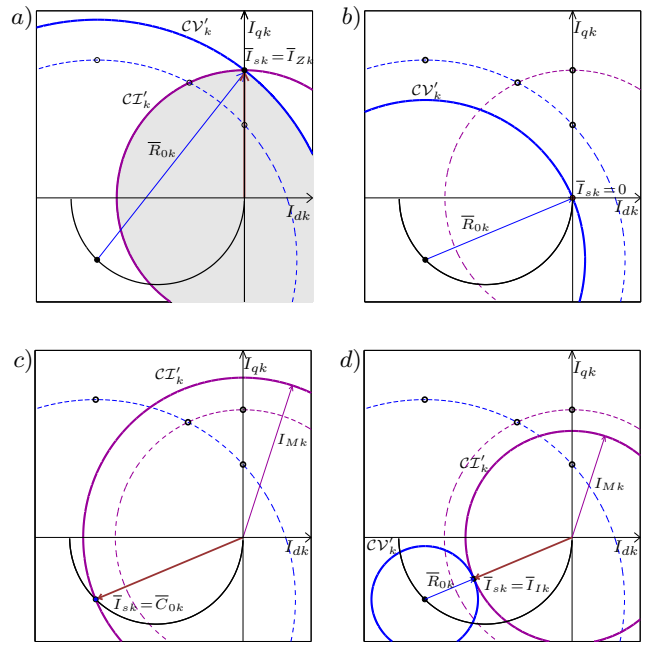


Fig. 7. Maximum current circles \mathcal{CV}_k and \mathcal{CI}_k in subspace Σ_{ω_k} obtained modulating the components V_{Mk} and I_{Mk} .

maximizes the scalar product $\mathbf{K}_\tau^T \mathbf{I}_M$ is obtained giving the maximum value $I_{\overline{M}}$ to the component I_{M3} related to the maximum component K_{q3} of vector \mathbf{K}_τ . The voltage vector \mathbf{V}_{Me} related to the current vector \mathbf{I}_{Me} is reported in Fig. 6.b.

Generalizing these two cases, four different constraints distribution into the subspaces $\bar{\Sigma}_{\omega_k}$ will be considered, see Fig. 7. The dashed lines are the voltage and current circles \mathcal{CV}_k and \mathcal{CI}_k showed in Fig. 4, while the solid lines are the new circles \mathcal{CV}'_k and \mathcal{CI}'_k obtained modulating the components V_{Mk} and I_{Mk} . In Fig. 7.a the operation point is $\bar{I}_{sk} = \bar{I}_{Zk} \equiv \bar{I}_{Ck} \equiv \bar{I}_{Ik}$, so the torque can be generated using only the quadrature component I_{qk} . Given the current constraint I_{Mk} and using equations (22) and (23), one obtains the component V_{Mk} :

$$V_{Mk} = |\bar{Z}_{sk}| \sqrt{X_{0k}^2 + (I_{Mk} - Y_{0k})^2}. \quad (27)$$

In Fig. 7.b the operation point is the origin $\bar{I}_{sk} = 0$ because $I_{Mk} = 0$, so the torque generated by subspace Σ_{ω_k} is zero. The component V_{Mk} has the following structure:

$$V_{Mk} = |\bar{Z}_{sk}| |\bar{C}_{0k}| = K_{qk} \omega_m. \quad (28)$$

In Fig. 7.c the operation point is $\bar{I}_{sk} = \bar{C}_{0k}$ because $V_{Mk} = 0$, so the torque generated by subspace Σ_{ω_k} is negative. The component I_{Mk} has the following structure:

$$I_{Mk} = |\bar{C}_{0k}| = K_{qk} \omega_m / |\bar{Z}_{sk}|. \quad (29)$$

In Fig. 7.d the operation point is $\bar{I}_{sk} = \bar{I}_{Ik} \equiv \bar{I}_{ik}$. Also in this case the torque generated by subspace Σ_{ω_k} is negative. Given the current constraint I_{Mk} , from (20) one obtains $R_{0k} + I_{Mk} = |\bar{C}_{0k}|$ and the component V_{Mk} is:

$$V_{Mk} = |\bar{Z}_{sk}| (|\bar{C}_{0k}| - I_{Mk}) = K_{qk} \omega_m - |\bar{Z}_{sk}| I_{Mk}. \quad (30)$$

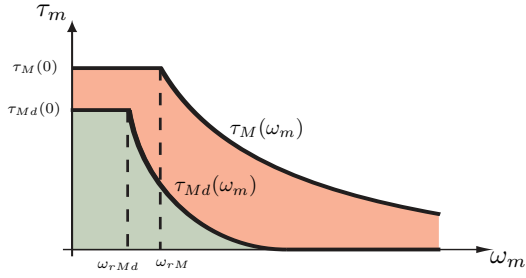


Fig. 8. Limit torques for a multi-phase synchronous motors.

These four cases show that when the operation point is defined, the components V_{Mk} and I_{Mk} are bounded by the equations (19) and (15).

VI. TORQUE CONTROL

Torque τ_m can be controlled by current vectors $\omega \bar{\mathbf{I}}_d$ in frame $\bar{\Sigma}_\omega$ not exceeding the constraints on the maximum input voltage and current. When $\omega \bar{\mathbf{I}}_d$ is constant, the condition $\omega \bar{\mathbf{I}}_s = \omega \bar{\mathbf{I}}_d$ can be achieved using the following control law:

$$\omega \bar{\mathbf{V}}_s = \omega \bar{\mathbf{Z}}_s \omega \bar{\mathbf{I}}_s + \omega \bar{\mathbf{K}}_\tau \omega_m - \mathbf{K}_c (\omega \bar{\mathbf{I}}_s - \omega \bar{\mathbf{I}}_d) \quad (31)$$

where $\mathbf{K}_c > 0$ is a control diagonal matrix and $\omega \bar{\mathbf{I}}_d$ is:

$$\omega \bar{\mathbf{I}}_d = \begin{cases} \omega \bar{\mathbf{I}}_M & \text{if } \tau_d \geq \tau_M(\omega_m) \\ \omega \bar{\mathbf{I}}_{cc} & \text{if } \tau_{Md}(\omega_m) < \tau_d < \tau_M(\omega_m) \\ \omega \bar{\mathbf{I}}_{md} & \text{if } 0 \leq \tau_d \leq \tau_{Md}(\omega_m) \end{cases} \quad (32)$$

where τ_d is the desired torque. $\tau_{Md}(\omega_m)$ is the maximum torque with minimum dissipation while $\tau_M(\omega_m)$ is the maximum torque. These two limit torques are function of the motor parameters, the voltage and current constraints and the control law. In Fig. 8 the two curves $\tau_{Md}(\omega_m)$ and $\tau_M(\omega_m)$ define three zones in the (τ_m, ω_m) torque plane: the green zone represents the region where the desired torque τ_d can be provided using the *minimum dissipation torque control*; the red zone represents the region where the torque τ_d is obtained using the *convex combination torque control*; the white zone is not allowed because τ_d cannot exceed the maximum torque τ_M , in this area the *maximum torque control is used*.

This control law, used together with relation (31), provides the desired torque τ_d satisfying the constraints (12), (13) and minimizing, when possible, the current dissipation.

A. Minimum dissipation torque control

The current constraint vector \mathbf{I}_M which minimizes the power dissipation is the vector with the minimum modulus parallel to vector \mathbf{K}_τ (see Fig. 5.a):

$$\mathbf{I}_M = \frac{\tau_d}{|\bar{\mathbf{K}}_\tau|} \hat{\mathbf{K}}_\tau = \frac{\mathbf{K}_\tau}{|\mathbf{K}_\tau|^2} \tau_d = \left[\begin{matrix} \tau_d \tilde{K}_k \\ \vdots \\ \tau_d \tilde{K}_k \end{matrix} \right]_{1:2:m_s-2} \quad (33)$$

where $\tilde{K}_k = \frac{K_{qk}}{|\omega \bar{\mathbf{K}}_\tau|^2} = k a_k / p \varphi_c \sqrt{\frac{m_s}{2} \sum_{k=1:2}^{m_s-2} (k a_k)^2}$ are the distribution coefficients of the current constraint \mathbf{I}_M into the subspaces $\bar{\Sigma}_{\omega k}$. Only the quadrature components I_{qk} of the current vectors $\bar{\mathbf{I}}_{sk}$ are used to generate torque (see

Fig. 7.a), therefore the current vector $\omega \bar{\mathbf{I}}_{md}$ which minimizes the power dissipation is:

$$\omega \bar{\mathbf{I}}_{md} = \left[\begin{matrix} j \tau_d \tilde{K}_k \\ \vdots \\ j \tau_d \tilde{K}_k \end{matrix} \right]_{1:2:m_s-2} = \frac{\omega \bar{\mathbf{K}}_{\tau N}}{|\omega \bar{\mathbf{K}}_{\tau N}|^2} \tau_d. \quad (34)$$

Note that the current vector $\omega \bar{\mathbf{I}}_{md}$ is parallel to the torque vector $\omega \bar{\mathbf{K}}_\tau$. Substituting (33) in (27) and using the voltage constraint (12), one obtains the following equation:

$$\sum_{k=1:2}^{m_s-2} \underbrace{|\bar{Z}_{sk}| \sqrt{X_{0k}^2 + (\tau_d \tilde{K}_k - Y_{0k})^2}}_{V_{Mk}} = V_M. \quad (35)$$

At low velocity the current constraint limits the torque. Using (33) and the current constraint (13) the maximum torque with minimum dissipation at low velocity is:

$$\tau_{Md}(0) = \mathbf{I}_M \left/ \sum_{k=1:2}^{m_s-2} \tilde{K}_k \right.$$

Substituting $\tau_{Md}(0)$ in (35) one obtains the rated velocity ω_{rMd} . When $\omega_m > \omega_{rMd}$, the limit torque decreases and it is limited by the voltage constraint. Given $\omega_m > \omega_{rMd}$, equation (35) can be numerically solved with respect to τ_d in order to obtain the maximum torque $\tau_{Md}(\omega_m)$ satisfying minimum dissipation and the voltage and current constraints. The desired torque τ_d can be obtained with minimum current vector $\omega \bar{\mathbf{I}}_{md}$ only if $\tau_d < \tau_{Md}(\omega_m)$. In Fig. 8 the curve $\tau_{Md}(\omega_m)$ defines the green zone representing the region where the desired torque τ_d can be provided minimizing the power dissipation.

B. Maximum torque control

The maximum torques $\tau_M(\omega_m)$ can be obtained maximizing the projection of the vector \mathbf{I}_M onto the torque vector \mathbf{K}_τ , see Fig. 6.a. To reach this goal it is necessary to sort the components K_{qk} of the vector \mathbf{K}_τ and apply the following current and voltage constraints distribution:

$$\begin{cases} I_{Mk} = I_M, & V_{Mk} = |\bar{Z}_{sG}| \sqrt{X_{0G}^2 + (I_M - Y_{0G})^2} & \text{if } k = G \\ I_{Mk} = |\bar{C}_{0k}|, & V_{Mk} = 0 & \text{if } k \in N_g \\ I_{Mk} = I_{Mg}, & V_{Mk} = K_{qk} \omega_m - |\bar{Z}_{sg}| I_{Mg} & \text{if } k = g \\ I_{Mk} = 0, & V_{Mk} = K_{qk} \omega_m & \text{if } k \in O_g \end{cases} \quad (36)$$

where $I_M = \mathbf{I}_M - \sum_{k \in N_g} |\bar{C}_{0k}| - I_{Mg}$ and:

- G is the index of the maximum component of \mathbf{K}_τ ,
- g is the index of the considered subspace univocally defined from the motor velocity ω_m (the reason will be explained later),
- N_g is the set of the subspaces already considered,
- O_g is the set of the subspaces not yet considered.

The subspace $\Sigma_{\omega G}$ related to the maximum component K_{qk} of the torque vector is shown in Fig. 4, the subspace $\Sigma_{\omega g}$ is shown in Fig. 7.d and the subspaces not yet considered and already considered are shown, respectively, in Fig. 7.b

and Fig. 7.c. Substituting the components V_{Mk} of (36) in the voltage constraint (12) one obtains the following equation:

$$\sum_{k \in [g, O_g]} K_{qk} \omega_m + |\bar{Z}_{sg}| \sqrt{X_{0G}^2 + (I_M - Y_{0G})^2} - |\bar{Z}_{sg}| I_{Mg} = V_M \quad (37)$$

Given ω_m , equation (37) can be rewritten as:

$$\sqrt{X_{0G}^2 + \left(I_M - \sum_{k \in N_g} |\bar{C}_{0k}| - I_{Mg} - Y_{0G} \right)^2} = \frac{V_M - \sum_{k \in [g, O_g]} K_{qk} \omega_m}{|\bar{Z}_{sg}|} + \frac{|\bar{Z}_{sg}|}{|\bar{Z}_{sg}|} I_{Mg}$$

This relation can be solved with respect to I_{Mg} obtaining the voltage V_{Mg} of the considered subspaces. The components \bar{I}_{sk} of the maximum current vector $\omega \bar{\mathbf{I}}_M$ are univocally defined from the constraints distribution (see Sec. IV):

$$\omega \bar{\mathbf{I}}_M = \begin{bmatrix} \bar{I}_{sk} \\ \vdots \\ \bar{I}_{sk} \end{bmatrix}_{1:2:m_s-2}, \quad \bar{I}_{sk} = \begin{cases} \max\{\bar{I}_{vk}, \bar{I}_{Ik}, \bar{I}_{Zk}\} \in \mathcal{C}_k & \text{if } k=G \\ X_{0k} + jY_{0k} & \text{if } k \in N_g \\ \bar{I}_{Ik} & \text{if } k=g \\ 0 & \text{if } k \in O_g \end{cases} \quad (38)$$

Note that $\Sigma_{\omega G}$ is the only subspace that generates torque because the current components in the other subspaces are negative or equal to zero.

When $\omega_m \leq \omega_{rM}$ the current constraint limits the torque and the maximum value I_M is given only by the subspace $\Sigma_{\omega k}$ related to the maximum component K_{qk} of vector \mathbf{K}_τ (see Case 2 of Sec.V), therefore $g = 0$, $N_g = \emptyset$ and in this case the equation (36) can be rewritten as:

$$\begin{cases} I_{Mk} = I_M, & V_{Mk} = |\bar{Z}_{sg}| \sqrt{X_{0G}^2 + (I_M - Y_{0G})^2} & \text{if } k=G \\ I_{Mk} = 0, & V_{Mk} = K_{qk} \omega_m & \text{if } k \in O_g \end{cases}$$

and the maximum torque at low velocity is:

$$\tau_M(0) = p\varphi_c \sqrt{\frac{m_s}{2}} G a_G I_M.$$

When the velocity ω_m increases the components V_{Mk} increase and there is a velocity ω_{rM} for which the voltage constraint is exactly satisfied. The rated velocity ω_{rM} can be obtained substituting the components V_{Mk} in (12). When $\omega_m > \omega_{rM}$ the voltage constraint limits the torque then it is necessary to redistribute the current constraint I_M into the other subspaces to reduce the components V_{Mk} , see (30). Since this operation causes a reduction of the torque (see vector I_{Mf} in Fig. 6.a), the current constraint I_M is redistributed only into the subspaces $\bar{\Sigma}_{\omega k}$ with $k \in [N_g, g]$ thus minimizing the torque reduction. The current and voltage constraints distribution (36) must be applied starting from the subspace $\Sigma_{\omega k}$ related to the minimum component K_{qk} up to the subspace $\Sigma_{\omega G}$. The index g is univocally defined by motor velocity ω_m : it is the first subspace $\Sigma_{\omega g}$ where $V_{Mg} > 0$. At the end, when $g = G$ and $O_g = \emptyset$, the equation (36) can be rewritten as:

$$\begin{cases} I_{Mk} = I_M - \sum_{k \neq G} |\bar{C}_{0k}|, & V_{Mk} = V_M & \text{if } k=G \\ I_{Mk} = |\bar{C}_{0k}|, & V_{Mk} = 0 & \text{if } k \in N_g \end{cases}$$

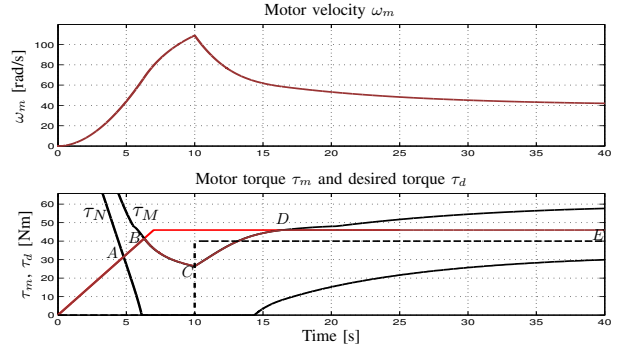


Fig. 9. Time behaviors of motor velocity ω_m , motor torque τ_m (brown), desired torque τ_d (red), external torque τ_e (magenta) and maximum torques τ_M and τ_N (black).

The maximum torque control is obtained choosing $\omega \bar{\mathbf{I}}_d = \omega \bar{\mathbf{I}}_M$ when $\tau_d \geq \tau_M(\omega_m)$. In Fig. 8 the curve τ_M defines the white region that represents the zone not allowed because τ_d cannot exceed the maximum torque.

C. Convex combination torque control

In Fig. 8 the curves τ_{Md} and τ_M define a red zone that represents the region where the two previous control laws cannot be used. In this region the optimal control law which satisfies the constraints (12), (13) and minimizes the current dissipation is quite complex and difficult to be found. In this case we propose the following suboptimal control law obtained as a convex combination of the maximum current vector $\omega \bar{\mathbf{I}}_M$, see (38), and the maximum current vector with minimum dissipation $\omega \bar{\mathbf{I}}_{Md} = \frac{\omega \bar{\mathbf{K}}_\tau}{|\omega \bar{\mathbf{K}}_\tau|^2} \tau_{Md}$, see (34). When $\tau_{Md} < \tau_d < \tau_M$ the torque τ_d is obtained using the following current vector:

$$\omega \bar{\mathbf{I}}_{cc} = \omega \bar{\mathbf{I}}_{Md} + \alpha (\omega \bar{\mathbf{I}}_M - \omega \bar{\mathbf{I}}_{Md})$$

$$\text{where } \alpha = \frac{\tau_d - \tau_N(\omega_m)}{\tau_M(\omega_m) - \tau_N(\omega_m)}.$$

VII. SIMULATION RESULTS

The simulation results described in this section have been obtained in Matlab/Simulink environment considering a motor with the following electrical and mechanical parameters: $m_s = 7$, $p = 1$, $R_s = 2 \Omega$, $L_s = 0.03$ H, $M_{s0} = 0.025$ H, $a_{M1} = 1$, $a_{M3} = 1/9$, $a_{M5} = 1/25$, $\varphi_r = 0.02$ Wb, $J_m = 1.6$ kg m², $b_m = 0.15$ Nm s/rad, $V_{max} = 100$ V, $I_{max} = 35$ A, $a_1 = 0.40$, $a_3 = 0.3$, $a_5 = 0.25$. The external torque τ_e is zero until $t = 10$ s then $\tau_e = 45$ Nm (see the black dashed line in Fig. 9). The time behaviors of motor velocity ω_m , motor torque τ_m , desired torque τ_d , external torque τ_e and maximum torques τ_M and τ_N are shown in Fig. 9 and the corresponding trajectories on the torque plane (τ_m, ω_m) are reported in Fig. 10. The letters A, B, C, D and E refer to the critical points for the control: A when $\tau_d = \tau_{Md}$, B and D when $\tau_d = \tau_M$, C when the external torque τ_e is applied and E the final steady-state condition. Note that for $\tau_d \leq \tau_M$, i.e. from point 0 to point B and from point D to point E, the control law (31) and (32) guarantees $\tau_m = \tau_d$. The constraints (12) and (13) are always satisfied as it is shown in Fig. 11. Fig. 12 shows the phase

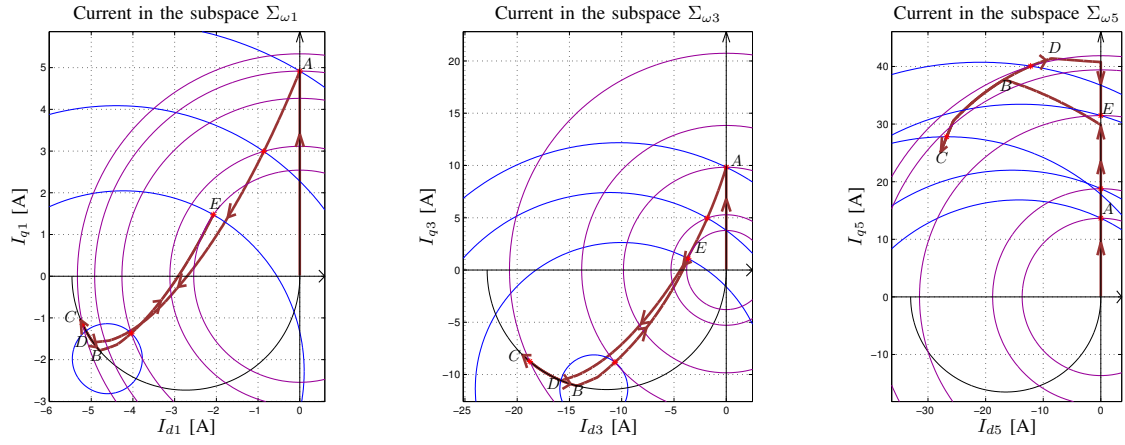


Fig. 13. Current and voltage circles CV_k , CI_k and current vectors \bar{I}_{sk} in the complex subspaces $\Sigma_{\omega k}$.

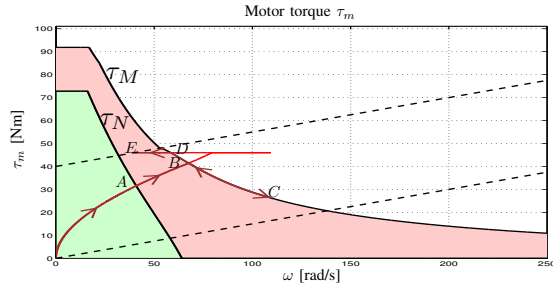


Fig. 10. Motor torque τ_m (brown), desired torque τ_d (red) and maximum torques τ_M and τ_N (black) as a function of motor velocity ω_m .

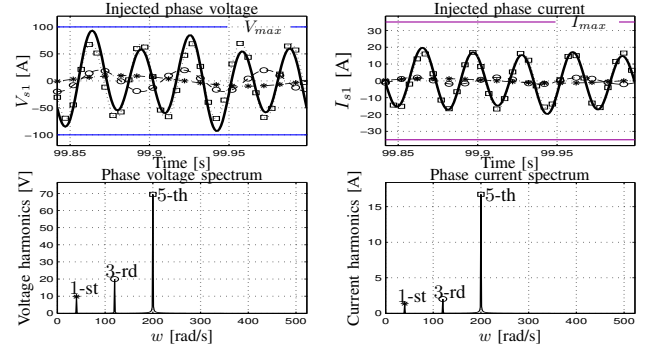


Fig. 12. Phase current and voltage waveform with their corresponding harmonic spectrum in steady-state condition.

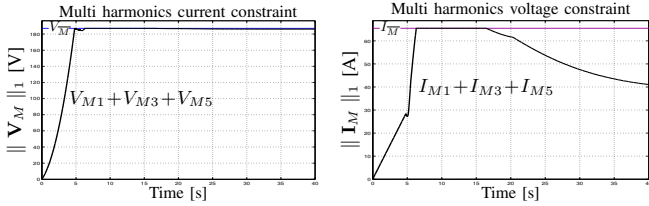


Fig. 11. Sum of the components V_{Mk} and I_{Mk} of vectors \mathbf{V}_M and \mathbf{I}_M .

current and voltage waveforms in the steady-state condition and their corresponding spectrum. It is clear that the phase voltage and phase current are obtained injecting the 1-st, the 3-rd and the 5-th harmonics. Moreover the obtained current and voltage waveforms satisfy (11). The current vectors \bar{I}_{sk} in the complex subspaces $\Sigma_{\omega 1}$, $\Sigma_{\omega 3}$ and $\Sigma_{\omega 5}$ are shown in Fig. 13. The desired torque τ_d is provided only by the quadrature components I_{qk} of the current vectors \bar{I}_{sk} until it is $\tau_d = \tau_N$ in point A. Note that from A to B, where the convex combination control $\omega_{I_{cc}}$ is used and the current vectors \bar{I}_{sk} remain within the intersection zones \mathcal{C}_k . From point B to point D the maximum torque control ω_{I_M} is used, the desired torque τ_d is generated only by the current component I_{q5M} . From D to E the desired torque τ_d is provided by the convex combination torque control.

VIII. CONCLUSIONS

In this paper a new vectorial approach to obtain the optimal current references considering the voltage and current constraints has been proposed. Since the number of phases, the impedance matrix and the rotor flux have been considered as design variables, the current references are as general

as possible. The optimality of the proposed control law is guaranteed when the minimum dissipation torque control or the maximum torque control are applied. Simulation results obtained in Simulink for a 7-phase motors validated the effectiveness of the presented control law.

REFERENCES

- [1] E. Semail, X. Kestelyn, A. Bouscayrol, "Right Harmonic Spectrum for the Back-Electromotive Force of a n -phase Synchronous Motor", Industry Applications Conference, 2004, 39th IAS Annual Meeting.
- [2] E. Levi, "Multiphase Electric Machines for Variable-Speed Applications" IEEE Trans. on Ind. Electronics, vol. 55, no. 5, May 2008.
- [3] L. Parsa, "On advantages of multi-phase machines" 31st Annual Conference of IEEE Industrial Electronics Society, IECON 2005.
- [4] L. Parsa and H.A. Toliyat, "Five-Phase Permanent-Magnet Motor Drives", IEEE Trans. on Industry Applications, 2005, Vol. 41, No. 1.
- [5] S. Xue, X. Wen, Z. Feng, "Multiphase Permanent Magnet Motor Drive System Based on A Novel Multiphase SVPWM", IPEMC 2006, Vol. 1.
- [6] F. Locment, E. Semail, X. Kestelyn, "Optimum use of DC bus by fitting the back-electromotive force of a 7-phase Permanent Magnet Synchronous machine", EPE 2005, Dresden, Germany, Sep. 2005.
- [7] L. Parsa, N. Kim, H.A. Toliyat, "Field Weakening Operation of a High Torque Density Five Phase Permanent Magnet Motor Drive", IEEE Int. Conference on Electric Machines and Drives, 15 May 2005.
- [8] R. Zanasi, M. Fei, "Saturated Vectorial Control of Multi-phase Synchronous Motors", NOLCOS 2010 - 8th IFAC Symposium on Nonlinear Control Systems, Bologna, Italy, 1-3 September 2010.
- [9] R. Zanasi, F. Grossi, M. Fei, "Complex Dynamic Models of Multi-phase Permanent Magnet Synchronous Motors", IFAC 2011, 18th IFAC World Congress, Milano, Italy, 28 Aug. - 2 Sept. 2011.
- [10] R. Zanasi, "The Power-Oriented Graphs Technique: system modeling and basic properties", VPPC 2010, Lille, France, Sept. 2010.
- [11] R. Zanasi, F. Grossi, "Multi-phase Synchronous Motors: POG Modeling and Optimal Shaping of the Rotor Flux", ELECTRIMACS 2008, Québec, Canada, 2008.